JOURNAL OF THERMOPHYSICS AND HEAT TRANSFER
Vol. 10, No. 1, January–March 1996

Shock-Tube Analysis of Argon Influence in Titan Radiative Environment

Laurent Labracherie,* Michel Billiotte,† and Lazhar Houas‡
Institut Universitaire des Systèmes Thermiques Industriels, 13397 Marseille, France

The effects of argon addition, in the range of 0–20% in a N_2–CH_4 mixture on the nonequilibrium radiation emitted behind a normal shock wave, have been investigated in a free-piston-driven shock tube. The intensity of spontaneous emission, for the $B^2\Sigma^+ \rightarrow X^2\Sigma^+$ electronic transition of CN molecules, is measured at a shock velocity of 5700 m/s propagating in a 200-Pa test gas mixture. Rotational and vibrational temperature profiles in the shock layer are obtained by matching three spectral lines simultaneously recorded in the $\Delta v = 0$ band with theoretical spectra calculations. The results show that the nonequilibrium radiation overshoot weakly increases with argon addition, whereas the equilibrium intensity value is not affected. The characteristic relaxation time of radiation is also affected so as to be reduced by argon addition. The vibrational relaxation time for CN molecules is also determined from the temperature profiles, but the accuracy is difficult to assess since the temperatures are weakly dependent functions of ratios of intensities.

Nomenclature

c = speed of light
F = rotational term, 1/cm
G = vibrational term, 1/cm
h = Planck's constant, J s
I = intensity of spontaneous emission, W/(cm^3 sr)
J = rotational quantum number
k = Boltzmann's constant, J/K
N = number density, 1/cm^3
n = electronic quantum number
Q_{tot} = total partition function
$q_{v'v''}$ = Franck–Condon factor
R_e = electronic transition moment
S_J = Hönl–London factor
T = temperature, K
v = vibrational quantum number
ν = wave number, 1/cm

Subscripts
e = electronic
r = rotational
v = vibrational

Superscripts
$'$ = upper state of transition
$''$ = lower state of transition

Introduction

THE next saturnine system exploration program, the so-called CASSINI mission, will integrate the launching and the landing of the Huygens probe through the Titan atmosphere.[1,2] Titan is Saturn's largest moon and is the only moon in the solar system with a substantial atmosphere. The previous saturnine missions, Voyager 1 and 2, gave most of the information about the composition of its atmosphere,[3,4] but the molar fractions of the three major species, N_2, CH_4, and probably Ar, are still not well defined.[5]

In the hypervelocity regime considered for the Huygens entry (about 6000 m/s), many complex processes take place behind the shock wave such as dissociation, vibrational, and electronic excitation of molecules, as well as weak ionization. Furthermore, these physical and chemical processes have the same time scale as the flow itself, so that the forebody shock layer is in thermochemical nonequilibrium. Because of the rapid dissociation of methane in the shock layer, CN molecules are formed in such proportions that a large part of the radiation is due to spontaneous emission for the $B^2\Sigma^+ \rightarrow X^2\Sigma^+$, CN electronic transition. It is now well known that the radiation is much stronger in the nonequilibrium region, which occurs soon after the shock, than it is in the equilibrium region of the downstream flow.[6,7] In previous experimental studies on nonequilibrium radiation phenomena in nitrogen flows,[8] the overshoot in radiation intensity was found to occur a finite distance away from the shock, unlike the theoretical prediction by the conventional one-temperature reaction scheme. The delay of the peak radiation is explained when the rate coefficients for dissociation reactions are assumed to be a function of both translational–rotational and vibrational temperatures.[9,10] Nowadays, the use of multitemperature models has been generalized for the numerical calculation of re-entry problems in Earth as well as in Mars atmospheres and has been also used for the Titan entry problem.[11–13]

A preliminary analysis has shown that the sensitivity of CN radiation to atmospheric composition is such that the accuracy of the N_2, CH_4, and especially Ar mole fractions in Titan atmosphere is too low to allow a safe design of the thermal protection system.[14] The previous studies were dedicated to test the sensitivity of the upstream compositions on the CN_v radiative heating by means of numerical simulations. Baillion and Taquin[15] have shown that the upstream chemical composition that leads to the maximum total radiative heat flux level is a 3% CH_4, 20% Ar, and 77% N_2 (in molar fraction) mixture. Experimental evidence of the choice of both the worst chemical upstream composition and the level of radiative heat flux was then to be verified in ground test facilities. A previous shock-tube study was carried out by Park and Bershader[11,16] in the combustion-driven shock tube at Stanford University with a 3% CH_4, 1% Ar, 95.7% N_2, and 0.3% H_2 upstream gas mixture at a velocity of nearly 6000 m/s. The authors compared their experimental results with a numerical simulation using a three-temperature model and a Millikan

Received May 9, 1995; revision received Sept. 20, 1995; accepted for publication Sept. 20, 1995.

*Research Assistant, UMR CNRS 139, Department of Two-Phase and Reactive Flows.
†Professor of Mechanics, UMR CNRS 139, Department of Two-Phase and Reactive Flows.
‡Research Scientist, UMR CNRS 139, Department of Two-Phase and Reactive Flows. Member AIAA.

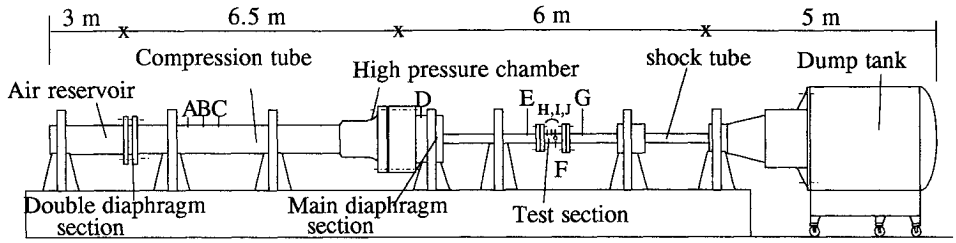

Fig. 1 Free-piston-driven shock-tube facility in Marseilles. A–G = pressure probe station and H–J = heat flux gauge station.

and White[17] relaxation formulation. Good agreement was found between experimental and theoretical results, but a few uncertainties remain, especially because of the large number of influencing parameters, which are not yet well defined, such as electron number density, electronic temperature, and collision cross sections, etc.

The present experimental study investigates the influence of argon addition, in the molar fraction range of 0–20% in the upstream N_2–CH_4 mixture, on the peak nonequilibrium radiation intensity of the CN violet $B^2\Sigma^+ \rightarrow X^2\Sigma^+$ electronic transition. The free-piston facility of the Marseilles laboratory is used to perform spectroscopic experiments downstream of a 5700-m/s incident normal shock wave at an initial pressure of around 200 Pa. The intensity of radiation behind the shock is recorded at three different wavelength during the same run. This simultaneous wavelengths recording technique of the time-dependent emission intensities is used to determine the rotational and vibrational CN temperatures within the nonequilibrium, one-dimensional shock layer. Acquisitions of the radiation spectrum have also been obtained by an optical multichannel analyzer in the equilibrium part of the flow.

Experimental Setup

Marseilles Free-Piston Facility: TCM2

The Marseilles hypersonic shock tunnel[18,19] was designed as part of the Hermes European space vehicle program in 1991. This facility operates in the reflected shock mode with a free-piston compression driver. The compensation process was initially used in aerothermodynamical studies by Stalker in the 1970s,[20] because incident shock Mach numbers of 10 can be obtained in the shock tube for a relatively high initial pressure of the test gas (up to 1 atm). The cancellation of the Hermes program was announced in 1993, and thus, the initial calibration of TCM2 was postponed. In radiation measurement experiments, an upstream pressure of up to 100 Pa is needed to achieve nonequilibrium effects with a significant level of spontaneous emission. In a free-piston-driven shock tube such as the Marseille facility, Mach number of 20 can be generated with an upstream pressure of the test gas higher than 1 kPa. A schematic of this facility is given in Fig. 1.

For these series of tests, the nozzle throat was removed and the 70-mm-i.d. shock tube was fitted with the test chamber located 3.5 m downstream of the main diaphragm. Typical velocities of the incident shock wave are about 5700 m/s with a 200-Pa initial pressure of the test gas. To generate these conditions, helium at an initial pressure of 3 atm in the compression tube is isentropically compressed by a 12-kg piston until the main diaphragm burst pressure of 17 MPa is reached. The facility operates in tuned conditions, i.e., the velocity of the piston at the time of rupture is sufficiently high (about 80 m/s) to maintain a constant driver pressure for a short time, and low enough so that the piston will gently stop before striking the end of the compression tube. However, considerable effort was made to design a specific device for the piston stop that prevents one from having to replace a part of the compression tube end in case of mismatch conditions. See the work of Dumitrescu[21] for a better description of this shock absorber device. The test chamber is fitted with a wall pressure probe, model PCB M113-A22, three platinum heat flux gauges for the shock velocity determinations, and two BK7 glass windows 20 mm in diameter. The internal wall of the test section of the shock tube was blackened by anodization to prevent prerecording of light before the shock arrives.

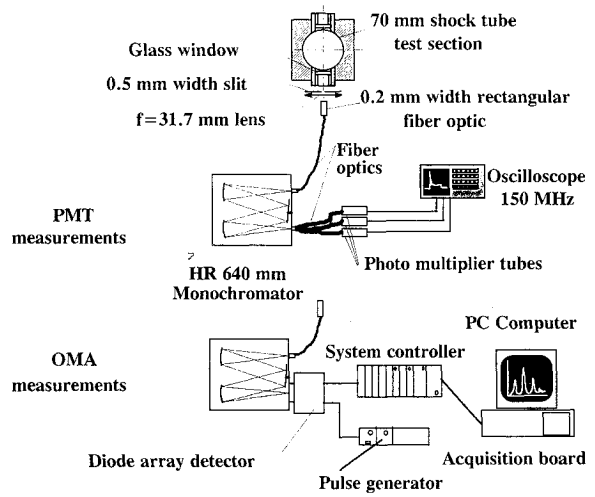

Fig. 2 Schematic of the collection optic arrangement and the measurement devices.

Optical Apparatus

A schematic of the optical apparatus for emission measurements is shown in Fig. 2. The emitted light is focused onto a rectangular fiber optic through a rectangular slit 0.5 mm wide by a 31.7 mm focal length lens. The solid angle of light collection is less than 0.001 sr and the spatial broadening at the center of the shock tube is about 0.8 mm. It would have been desirable to reduce this value because the spatial widening can appreciably affect the shape of the emission signal, but in so doing, the signal-to-noise ratio deteriorates to an unacceptable value. The reception fiber optic, which is 0.2 mm wide and 5 mm high, is imaged on the entrance slit of a Czerny–Turner 640-mm monochromator (Jobin–Yvon HR640). The dimension of the grating is 10 × 10 cm, ruled to 3000 lines/mm; thus, the linear dispersion is about 3.7 Å/mm at 4000 Å.

Two emission measurement devices are available for the intensity measurement at the exit of the monochromator: 1) a time-evolution emission intensity measurement with photomultiplier tubes (PMT, Hamamatsu R105UH) and 2) a single spectrum acquisition with an optical multichannel analyzer (OMA). The time-dependent intensity of radiation is simultaneously recorded at three wavelengths with a special apparatus at the monochromator exit. This system, shown in Fig. 3, is achieved by means of rectangular bundle of 0.2-mm fiber optics. The width of each of the three slits is 0.2 mm and the horizontal spacing between the slits has been fixed to match with three spectral wavelengths of interest. This device is particularly attractive in reducing the number of runs needed because the three scanned wavelengths correspond to

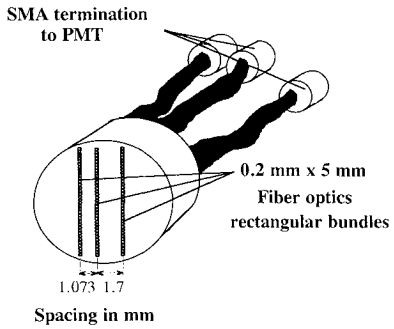

Fig. 3 Exit slit system for the monochromator. This arrangement allows measurement of the emission signal at three different wavelengths during a shot.

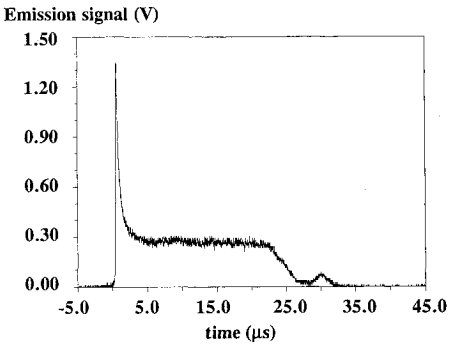

Fig. 4 Typical evolution of CN emission intensity recorded at 3880 Å behind a 5700-m/s shock wave propagating in a 200-Pa N_2–CH_4 mixture.

identical experimental conditions. Each of the three fiber optics guide the light towards the photocathodes of three identical PMTs whose voltages are recorded and stored on a Tektronix 150-MHz bandwidth oscilloscope with a 100 Msamples/s recording. Because of the low signal levels, PMT amplifying circuits have been designed to produce a current/voltage conversion of 4 mV/μA on a 50-Ω load resistance.[22] Unfortunately, the amplifying circuits increase the response time of the PMTs by two orders of magnitude, or to about 50 ns.

The OMA apparatus consists of a 1024-elements diode array (intensified IRY 1000, Princeton Instruments), an MCP intensifier, and a system controller. The system controller (Jobin–Yvon, model Spectralink and PRISM software) sets the total integration time of the detector and reads the charge from each of the diodes after light integration. In gated mode, the diode array operates in recording mode as long as a pulse of voltage, generated by a pulser (Princeton PG-10) and triggered by one of the platinum heat flux gauges, is applied to the intensifier. The data are read and transferred to the computer memory after the total exposure time (including the gate time). The time between two acquisitions, limited by the computer clock, cannot be less than 0.15 s so that only one single spectrum can be recorded during a shot. The delay and the duration of the gate pulse can be tuned to account for situations in which the spectrum is to be measured in the equilibrium, or in the nonequilibrium region. The spectral calibration and the slit function measurement of the PMT and the OMA devices are performed using one of the narrow lines emitted by a low-pressure spectral lamp. The accuracy in the spectral calibration of the grating is limited both by the width of the exit slit fiber for the PMT measurement system and by the area of the diode element in the OMA device. The error on the value of the reference wavelength is about 0.15 Å.

Results

A typical PMT signal of CN emission at 3880 Å is shown in Fig. 4. The radiation rises very rapidly because of the fast electronic excitation processes. Then the intensity of radiation decreases until an equilibrium value is reached. The test ends when the contact surface crosses the test section. Such a nonequilibrium radiation profile exhibits three characteristic parameters: 1) the time to reach the peak in radiation intensity, 2) the time to reach the equilibrium plateau, and 3) the ratio of nonequilibrium-to-equilibrium radiative heat flux. The experimental determination of the time to reach the maximum in intensity is limited by the response time of the whole detection apparatus: the spatial resolution at the center of the test section and the response function of the PMT conditioning circuit tend to increase this time. The global transfer function was estimated to be a Gaussian shape with a 100-ns bandpass. Unfortunately, the deconvolution process considerably amplifies the noise present in the signals so that accurate results cannot be obtained by using such data processing.

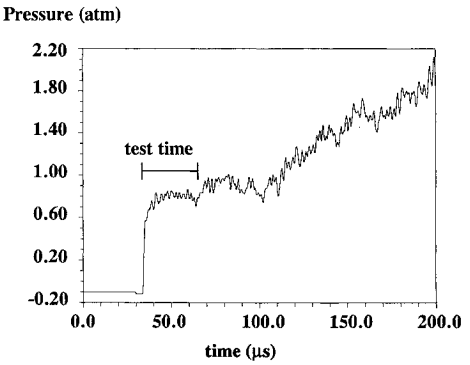

Fig. 5 Record of the pressure behind the shock. Test conditions are 202 Pa, 5590 m/s, and 5% Ar.

The determination of the two other parameters related to the establishment of equilibrium is limited by both the boundary-layer development and the vanishing of the signal caused by the arrival of the contact surface. In free-piston shock-tube experiments, the test time is greatly enhanced by the compression of the driver gas during the shock propagation. Figure 5 shows a typical record of the pressure evolution downstream of the shock. The test time, i.e., the time duration of constant pressure, is about 25 μs, which corresponds to a distance of 15 cm at the test conditions. The boundary-layer development should be considered for the determination of intensity at the equilibrium distance: the rotational, vibrational, and electronic temperatures and the density continuously increase with distance behind the shock front,[23] so that the CN emission will rise more rapidly than theory would predict. In the shock-tube radiation measurements of Arnold and Nicholls,[24] the application of the Mirels boundary-layer theory accounts for about one-third of the difference between the theoretical and experimental emission curves for tests at 3500 K and a shock velocity of 2900 m/s. However, for their tests at 8000 K and 5800 m/s, the rise in temperature induced by the boundary-layer effects causes the CN to dissociate so that the emission only slightly increases. The weak influence of the boundary-layer growth at our test conditions was also confirmed by computing the intensity of radiation with the rotational, vibrational, and electronic temperatures and density evolution corrected for boundary-layer effects.[25]

Effects of Argon Addition on CN Emission

To evaluate the effect of argon addition in a N_2–CH_4 upstream mixture on the nonequilibrium intensity of spontaneous emission, four different upstream gas mixtures were tested. The initial argon composition was varied from 0 to 20%, while the methane molar fraction was fixed at 3%, whatever the mixture. The four test mixture compositions

Table 1 Composition in molar fractions of the four test gas mixtures

Mixture	Composition, ±10 ppm Ar, %	CH_4, %	N_2, %
1	0	3	97
2	5	3	92
3	10	3	87
4	20	3	77

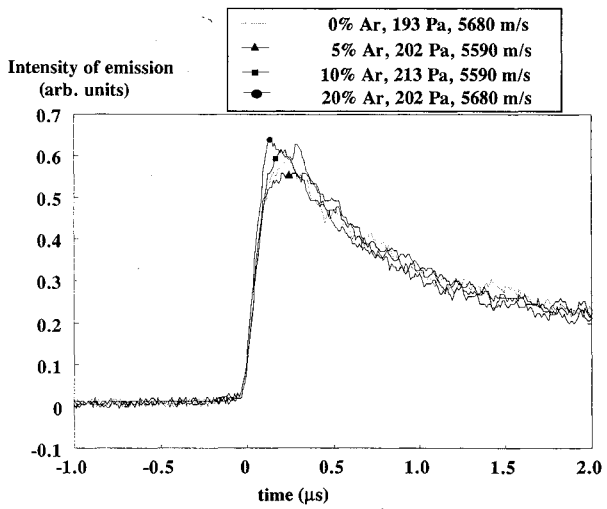

Fig. 6 Comparison of peak intensity of spontaneous emission for the four upstream mixtures with corresponding composition, initial pressure, and shock velocity.

used in the present study are summarized in Table 1. To limit the introduction of impurities in the test gas, a primary vacuum of 0.1 Pa is achieved in the shock tube; then the introduction of the test gas at atmospheric pressure is carried out, followed by another 0.1-Pa vacuum; finally, the shock tube is filled up with test gas to the desired initial pressure. The shock speed measurement is achieved by recording the time-of-flight between the three platinum heat flux gauges located at the test chamber wall. The error on the shock velocity is about 200 m/s and the error on the initial pressure of the test gas mixture is 1 Pa. The reproducibility of test conditions was evaluated by comparing the radiation profiles at the same initial test conditions. The difference between radiation profile intensities was never found to be up to 3% for a same upstream composition.

The comparison of radiation intensity profiles, recorded at 3882 Å for each of the four upstream mixtures, is shown in Fig. 6. The peak intensity ranges, in arbitrary units, from 0.56 for the 5% Ar mixture, to 0.64 for the 20% Ar mixture, for a maximum relative variation of roughly 10%. The time to reach the maximum in intensity is not influenced by argon addition. Unfortunately, the presence of oscillations in the signal could lead to an underestimate of the value of the peak intensity. CN excited states are populated by collisional processes with electrons, atoms, or/and molecules. Collisional electronic transitions are much more likely to occur if the masses of the two particles are nearly equal. When the colliding particle is a free electron, its kinetic energy can be transferred more efficiently to a bound electron, thereby raising its orbit.[7] In the range of the temperature considered here, a weak ionization of the atoms present in the downstream mixture is to be expected (the maximum degree of ionization is about 1%); thus, the argon addition leads to an increase in the number of free electrons formed by collisional ionization processes so that the spontaneous emission intensity will increase. The characteristic excitation time is about 250 ns, but no evidence of time increasing with argon addition was observed from the four different emission records. However, the response time of the apparatus should be reduced to under 10 ns for a correct measurement of the emission excitation time.

In Fig. 7, the emission profiles are shown for the whole record duration. The main effect of argon addition is the rise in duration of the plateau of radiation. Thus, the intensity of radiation seems to reach an equilibrium value faster when more argon atoms are present in the mixture. Under the conditions of interest in the present experiment, translational, rotational, and vibrational relaxation are fast compared to the rates of chemical reactions in the gas. Thus, the radiation decay time represents the chemical adjustment of the gas since all degrees of freedom of the molecules are in thermodynamic equilibrium. Therefore, if more heavy argon atoms are present in the shock layer, faster dissociation of CN molecules by means of collisional processes is to be expected.

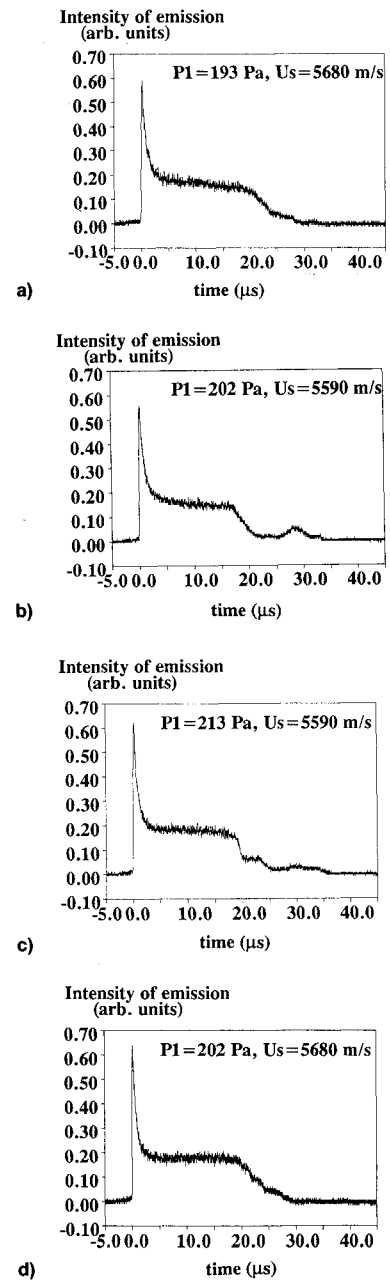

Fig. 7 Comparison of equilibrium intensities of spontaneous emission for the different upstream mixtures: a) 0%, b) 5%, c) 10%, and d) 20% Ar.

Determination of Rotational and Vibrational Temperatures

The spontaneous emission intensity of a single rotational line of the CN transition, produced by excitation behind the shock wave, is given by[26]

$$I^{n',v',J'}_{n'',v'',J''} = \frac{64\pi^4 c\nu^4}{3} |R_e|^2 q_{v'v''} \frac{S_{J'}}{2J' + 1} N(n', v', J') \quad (1)$$

where the set of quantum numbers n', v', and J' is associated, respectively, with the electronic, vibrational, and rotational levels of the upper $B^2\Sigma^+$ state. A similar meaning applies to the quantum numbers n'', v'', and J'' of the lower $X^2\Sigma^+$ state. $|R_e|^2$ is the sum of the squares of the components of the electronic transition moment at the (v', v'') vibrational band to which the J' and J'' rotational lines belong. $N(n', v', J')$ is the number of excited-state molecules and ν is the wave number of the transition given by the term value difference:

$$\nu = \nu_e' - \nu_e'' + G(n', v') - G(n'', v'') + F(n', v', J') - F(n'', v'', J'') \quad (2)$$

Because of the excitation conditions existing behind the shock wave, it is appropriate to write the number of excited-state molecules as the product of three Boltzmann factors, for each of the electronic, vibrational, and rotational degrees of freedom, each of which has its own effective excitation temperature, T_e, T_v, and T_r, respectively. It can be shown that the assumption of equilibrium between the different electronic excited-states is fully justified in the case of the CN electronic levels $B^2\Sigma^+$ and $A^2\Pi_i$.[16] Thus, the number density $N(n', v', J')$ is

$$N(n', v', J') = \frac{N_0(2J' + 1)}{Q_{\text{tot}}} \times \exp\left\{\frac{-hc}{k}\left[\frac{F(n', v', J')}{T_r} + \frac{G(n', v')}{T_v} + \frac{\nu_e'}{T_e}\right]\right\} \quad (3)$$

The intensity of $I(\nu)$ at a given wavelength number is then

$$I(\nu) = \sum_{\substack{\text{bands} \\ \text{lines}}} I^{n',v',J'}_{n'',v'',J''} b(\nu) \quad (4)$$

where $b(\nu)$ is the Voigt profile function that takes into account Doppler (temperature) and pressure broadening of the rotational line. The theoretical spectrum obtained has to be convoluted with the experimental slit function to allow a direct comparison of the calculated spectrum with the measured one. The CN spectrum is computed using the program developed by Arnold and Whiting.[26] The values of the spectroscopic constants for the $B^2\Sigma^+ \rightarrow X^2\Sigma^+$ electronic transition are taken partly from Herzberg,[27] Spinder,[28] and Hornkohl et al.[29]

Theoretically, the ratio of two intensities in the same vibrational band is only a function of the rotational temperature. The vibrational temperature can be determined similarly by measuring two intensities in different vibrational bands: the ratio of these two intensities depends only on the rotational and vibrational temperatures. However, the overlapping of the different bands and the slit function of the instrument prevent obtaining a discrete relationship between the ratios of the measured intensities and the temperatures.[29-31] The temperature dependence of intensity ratios, calculated for a slit function passband of 1 Å, is shown in Fig. 8: the ratio of $I_{(3879.7\text{Å})}$ and $I_{(3875.8\text{Å})}$, which belong both to the same vibrational band $(v', v'') = (0, 0)$, depends only on the rotational temperature and the ratio of $I_{(3879.7\text{Å})}$ and $I_{(3869.6\text{Å})}$, which belong, respectively, to the (0, 0) and (1, 1) band, is only a function of the rotational and vibrational temperatures. Unfortunately, above 5000 K the weak dependence of the ratios with temperature decreases the accuracy in the determination of temperature.

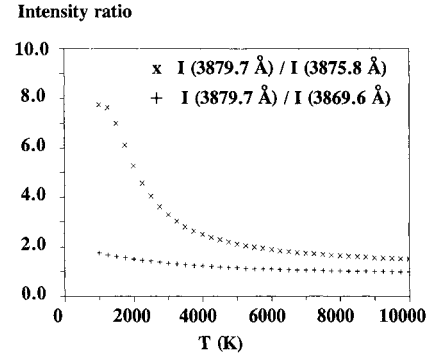

Fig. 8 Calculated intensity ratios for equilibrium temperatures from 0 to 10,000 K. The two intensities $I_{(3879.7\text{Å})}$ and $I_{(3875.8\text{Å})}$ belong to the $(v', v'') = (0, 0)$ band and $I_{(3869.6\text{Å})}$ to the (1, 1) band of the CN violet system.

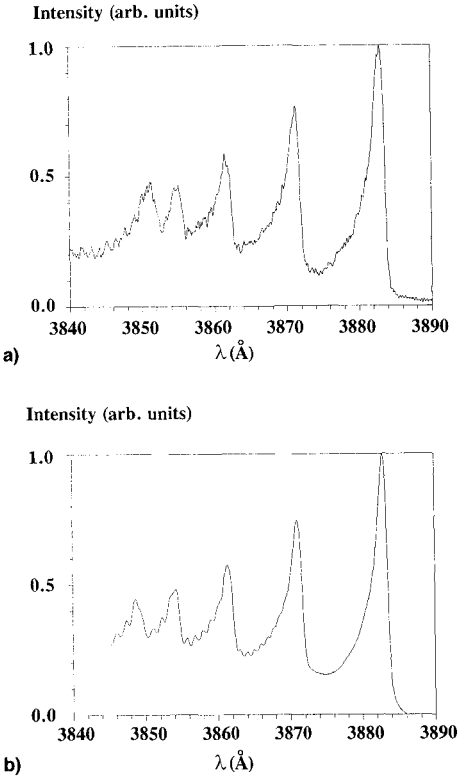

Fig. 9 Comparison of a) experimental and b) theoretical spectra for equilibrium conditions (calculated for an equilibrium temperature of 7800 K).

Figure 9a shows the CN violet emission spectrum from 3840 to 3890 Å, recorded by OMA detection in the equilibrium region of the shock layer. The accumulation time of the diode array corresponds to a gate pulse width of 3 μs. The temperature is determined from a comparison between the computed and the measured spectra. In other words, the temperature is iterated until the calculated spectrum best fits the experimental one. The value of the equilibrium temperature is found to be 7800 ± 600 K and is in good agreement with theoretical calculation.[13,25] The theoretical spectrum is shown in Fig. 9b.

Figure 10 shows the ratios of the three intensities (3869.6, 3875.8, and 3879.7 Å) measured for a run with the 20% argon test mixture at a shock velocity of 5680 m/s with an initial pressure of 210 Pa. The temperature profiles calculated from these intensity ratios are shown in Fig. 11. The error on the

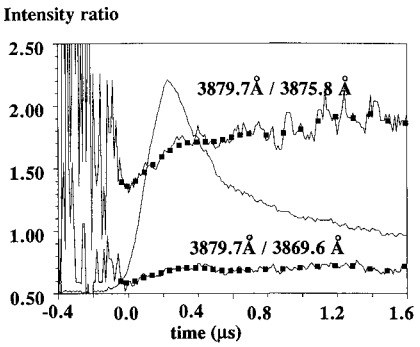

Fig. 10 Ratios of experimental intensities $I_{(3879.7Å)}/I_{(3875.8Å)}$ and $I_{(3879.7Å)}/I_{(3869.6Å)}$. The plot squares represent the smoothed values used for the temperature determination. One emission signal is shown for time comparison.

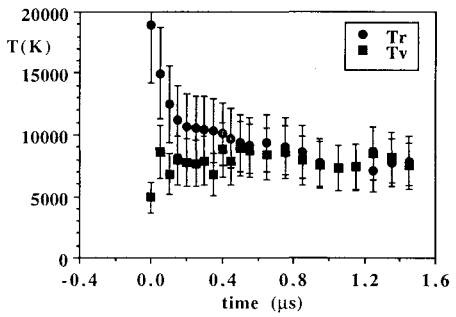

Fig. 11 Rotational and vibrational temperatures determined from ratios of experimental intensities of spontaneous emission (0% Ar, 193 Pa, and 5680 m/s).

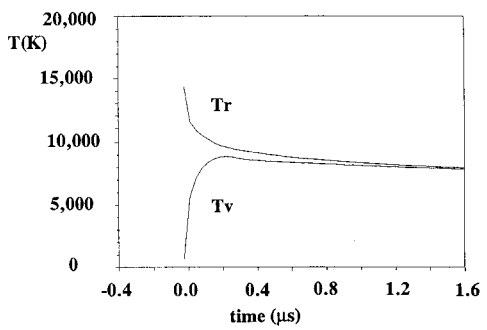

Fig. 12 Numerical results of rotational and vibrational temperatures; 0% Ar, 193 Pa, and 5680 m/s (courtesy of Kossi Koffi-Kpante[25]).

rotational temperature determination is at least 15% and the error may be up to 50% for the vibrational temperature. In the accuracy of the measurements, the temperatures are not sensitive to argon addition. The temperatures calculated using a three-temperature model[25] including vibration–dissociation coupling and Millikan and White relaxation laws are plotted for comparison in Fig. 12. The initial conditions for this computation were set exactly to the experimental values of the present experiment. The measured equilibrium value of the temperature is about 8400 K and the calculated one is 7700 K. On the other hand, in the nonequilibrium part of the downstream flow, the measured and calculated temperatures diverge, especially close to the shock. The poor agreement in this region is mainly due to the weak temperature dependence of intensities ratios at temperatures above 10,000 K. The measured vibrational relaxation time is about 500 ns, twice the value calculated with the theoretical Millikan and White formula[17] at a temperature of 10,000 K. The spatial broadening of the radiation measurement at the center of the test section accounts for this discrepancy.

The simultaneous wavelength measurement technique allows the determination of both the rotational and vibrational temperatures. However, the accuracy is limited by factors such as the weak level of the emission signal, the response time of the photomultipliers, and the errors of the wavelength positioning. On the other hand, with OMA measurements the error in temperature determination is decreased, but only time-frozen intensity measurements can be achieved. In high-speed radiation measurements, the use of rapid multichannel acquisition systems such as streak cameras would provide more accurate nonequilibrium data since sweep speeds of about 10 ns are available with the existing technology.

Conclusions

The effect of argon addition, ranging from 0 to 20% in a N_2–3% CH_4 upstream mixture, on the CN emission behind a normal shock has been studied at a shock velocity of 5700 m/s. The nonequilibrium emission intensity overshoot just behind the shock slightly increases with argon addition, whereas the plateau of equilibrium radiation is not affected. The characteristic relaxation time of radiation, which represents the chemical adjustment of the gas, was found to decrease with argon addition. Rotational and vibrational temperatures for CN have been determined from a comparison between measured and computed intensities of emission in the $\Delta v = 0$ part of the violet system. Temperatures in the equilibrium part of the flow obtained both from OMA and three wavelengths recording diagnostics are close to numerical three-temperature calculations. In the nonequilibrium region, there is a fair agreement between the measured and calculated temperature profiles. This region requires a more detailed spatial resolution and accurate analysis to obtain further information about molecular behavior. Furthermore, the accuracy would be appreciably increased with hf amplifiers of typical rise time in the range of 10 ns.

However, the present experiment confirms the choice of the 20% Ar–3% CH_4–77% N_2 mixture as the most radiative atmosphere for the Huygens probe.

Acknowledgments

This study was realized through the financial support of the Aerospatiale Company, under Contract 250064-32319Z, represented by Marc Baillion. We express our thanks to Alain Canova for his competent operation of the free-piston facility and auxiliary equipment.

References

[1]Scoon, G. E. N., "Cassini—A Concept for Titan Probe," European Space Agency Bulletin 41, Feb. 1985, pp. 19, 20.

[2]Scoon, G. E. N., and Flury, W., "Cassini Mission—The Titan Probe," International Astronautical Federation Paper 87-445, Oct. 1987.

[3]*Science*, Vol. 212, April 10, 1981.

[4]*Science*, Vol. 215, Jan. 29, 1982.

[5]Hunten, D. M., Tomasko, M. G., Flasar, F. M., Samuelson, R. E., Strobel, D. F., and Stevenson, D. J., *Saturn*, edited by Gehrels and Mildred, Univ. of Arizona Press, Tucson, AZ, 1984.

[6]Park, C., "Assessment of a Two-Temperature Kinetic Model for Dissociating and Weakly Ionizing Nitrogen," *Journal of Thermophysics and Heat Transfer*, Vol. 2, No. 1, 1988, pp. 8–16.

[7]Park, C., *Nonequilibrium Hypersonic Aerothermodynamics*, Wiley, New York, 1990.

[8]Allen, R. A., "Non Equilibrium Shock Front Rotational, Vibrational, and Electronic Temperature Measurements," AVCO-Everett Research Lab., Res. Rept. 186, Everett, MA, Aug. 1964.

[9]Park, C., "Review of Chemical Kinetic Problems of Future NASA Mission, I: Earth Entries," *Journal of Thermophysics and Heat Transfer*, Vol. 7, No. 3, 1993, pp. 385–398.

[10]Park, C., "Review of Chemical Kinetic Problems of Future NASA Mission II: Mars Entries," *Journal of Thermophysics and Heat Transfer*, Vol. 8, No. 1, 1993, pp. 9–23.

[11]Park, C. S., and Bershader, D., "Studies of Radiative Emission

from the Simulated Shock Layer of the Huygens Probe," *Proceedings of the 18th International Symposium on Shock Waves* (Sendai, Japan), 1991, pp. 671–676.

[12]Baillion, M., Taquin, G., and Soler, J., "Huygens Radiative Probe Environment," *Proceedings of the International Union of Theoretical and Applied Mechanics* (Marseille, France), 1992, pp. 13–20.

[13]Baillion, M., Taquin, G., and Soler, J., "Huygens Radiative Probe Environment," *Proceedings of the 19th International Symposium on Shock Waves* (Marseille, France), 1993, pp. 339–346.

[14]Nelson, H. F., "Feasibility of Determining Haze Properties During High-Speed Titan Entry," *Journal of Thermophysics and Heat Transfer*, Vol. 8, No. 3, 1994, pp. 486–493.

[15]Baillion, M., and Taquin, G., "Huygens Probe: Aerodynamic and Aerothermodynamic Design," *Proceedings of the 2nd European Symposium on Aerothermodynamics for Space Vehicles*, European Space Agency, SP-367, Noordwijk, The Netherlands, 1994.

[16]Park, C. S., "Studies of Radiative Emission from the Simulated Shock Layer of the Huygens Probe," Ph.D. Dissertation, Stanford Univ., Stanford, CA, 1991.

[17]Millikan, R. C., and White, D. R., "Systematics of Vibrational Relaxation," *Journal of Chemical Physics*, Vol. 39, Dec. 1963, pp. 3209–3213.

[18]Brun, R., Burtschell, Y., Dumitrescu, L. Z., Dumitrescu, M. P., Houas, L., Labracherie, L., and Zeitoun, D., "Computation and Experimentation of Free-Piston Shock Tunnels: Example of the Marseille Facility," *New Trends in Instrumentation for Hypersonic Research*, edited by A. Boutier, NATO-ASI, Kluwer Academic, Norwell, MA, 1992.

[19]Labracherie, L., Dumitrescu, M. P., Burtschell, Y., and Houas, L., "On the Compression Process in a Free-Piston Shock Tunnel," *Shock Waves Journal*, Vol. 3, No. 1, 1993, pp. 19–23.

[20]Stalker, R. J., "A Study of the Free-Piston Shock Tunnel," *AIAA Journal*, Vol. 5, No. 12, 1967, pp. 2160–2167.

[21]Dumitrescu, M. P., "Performances et Fonctionnement de la Soufflerie Hypersonique TCM2," Ph.D. Dissertation, Univ. of Provence, Marseille, France, 1994.

[22]Labracherie, L., "Détermination des Températures Rotationnelles et Vibrationnelles de CN à l'Aval d'un Choc Droit se Propageant dans une Atmosphère de Titan Reconstituée," Ph.D. Dissertation, Univ. of Provence, Marseille, France, 1994.

[23]Mirels, H., "Test Time in Low-Pressure Shock Tubes," *Physics of Fluids*, Vol. 6, No. 9, 1963, pp. 1201–1214.

[24]Arnold, J. O., and Nicholls, R. W., "A Shock Tube Determination of the CN Ground State Dissociation Energy and the CN Violet Electronic Transition Moment," *Journal of Quantitative Spectroscopy and Radiative Transfer*, Vol. 13, 1973, pp. 115–133.

[25]Kpante, K., Zeitoun, D., and Labracherie, L., "Computation and Experimental Validation of N_2-CH_4-Ar Mixtures Nonequilibrium Shock Layer," *Shock Wave Journal* (submitted for publication).

[26]Arnold, J. O., Whiting, E. E., and Lyle, G. C., "Line by Line Calculation of Spectra from Diatomic Molecules and Atoms Assuming a Voigt Line Profile," *Journal of Quantitative Spectroscopy and Radiative Transfer*, Vol. 9, 1969, pp. 775–798.

[27]Herzberg, G., *Molecular Spectra and Molecular Structure. I. Spectra of Diatomic Molecules*, 2nd ed., Vol. 1, Van Nostrand, New York, 1950.

[28]Spindler, R. J., "Franck-Condon Factors Based on RKR Potentials with Applications to Radiative Absorption Coefficients," *Journal of Quantitative Spectroscopy and Radiative Transfer*, Vol. 5, 1965, pp. 165–204.

[29]Hornkohl, J. O., Parigger, C., and Lewis, J. W., "Temperature Measurements from CN Spectra in a Laser-Induced Plasma," *Journal of Quantitative Spectroscopy and Radiative Transfer*, Vol. 46, No. 5, 1991, pp. 405–411.

[30]Blackwell, H. E., and Scott, C. D., "Nonequilibrium Shock Layer Temperature Profiles from Arc Jet Radiation Measurements," AIAA Paper 89-1679, June 1989.

[31]Labracherie, L., Billiotte, M., and Houas, L., "Nonequilibrium Determination of Temperature Profiles by Emission Spectroscopy," *Journal of Quantitative Spectroscopy and Radiative Transfer*, Vol. 54, No. 3, 1995, pp. 573–579.